Inorg. Chem. **2003**, *42*, 6274–6283

Catalytic Oxidation of 3,5-Di-*tert*-butylcatechol by a Series of Mononuclear Manganese Complexes: Synthesis, Structure, and Kinetic Investigation

Michael U. Triller,[†] Daniel Pursche,[†] Wen-Yuan Hsieh,[‡] Vincent L. Pecoraro,*[,‡] Annette Rompel,*[,§] and Bernt Krebs*[,†]

Institut für Anorganische und Analytische Chemie der Westfälischen Wilhelms-Universität Münster, Wilhelm-Klemm-Strasse 8, 48149 Münster, Germany, Institut für Biochemie der Westfälischen Wilhelms-Universität Münster, Wilhelm-Klemm-Strasse 2, 48149 Münster, Germany, and Department of Chemistry, The University of Michigan, Ann Arbor, Michigan 48109-1055

Received July 7, 2003

The manganese compounds $[Mn(bpia)(OAc)(OCH_3)](PF_6)$ (**1**), $[Mn(bipa)(OAc)(OCH_3)](PF_6)$ (**2**), $[Mn(bpia)(Cl)_2](ClO_4)$ (**3**), $[Mn(bipa)(Cl)_2](ClO_4)$ (**4**), $[Mn(Hmimppa)(Cl)_2]\cdot CH_3OH$ (**5**), and $[Mn(mimppa)(TCC)]\cdot 2CHCl_3$ (**6**) (bpia = bis(picolyl)(*N*-methylimidazole-2-yl)amine; bipa = bis(*N*-methylimidazole-2-yl)(picolyl)amine; Hmimppa = ((1-methylimidazole-2-yl)methyl)((2-pyridyl)methyl)(2-hydroxyphenyl)amine; TCC = tetrachlorocatechol) were synthesized and characterized by various techniques such as X-ray crystallography, mass spectrometry, IR, EPR, and UV/vis spectroscopy, cyclic voltammetry, and elemental analysis. **1** and **2** crystallize in the triclinic space group $P\bar{1}$ (No. 2), **4** and **6** crystallize in the monoclinic space group $P2_1/n$ (No. 14), and **5** crystallizes in the orthorhombic space group $Pna2_1$. Complexes **1**–**4** are structurally related to the proposed active site of the manganese-dependent extradiol-cleaving catechol dioxygenase exhibiting an N_4O_2 donor set (**1** and **2**) or N_4Cl_2 donor set (**3** and **4**). Cyclic voltammetric data show that the substitution of oxygen donor atoms with chloride causes a shift of redox potentials to more positive values. These compounds show high catalytic activity regarding the oxidation of 3,5-di-*tert*-butylcatechol to 3,5-di-*tert*-butylquinone exhibiting saturation kinetics at high substrate concentrations. The turnover numbers $k_{cat} = (86 \pm 7)\ h^{-1}$ (**1**), $k_{cat} = (101 \pm 4)\ h^{-1}$ (**2**), $k_{cat} = (230 \pm 4)\ h^{-1}$ (**3**), and $k_{cat} = (130 \pm 4)\ h^{-1}$ (**4**) were determined from the double reciprocal Lineweaver–Burk plot. Compounds **5** and **6** can be regarded as structural and electronic Mn analogues for substituted forms of Fe-containing intradiol-cleaving catechol dioxygenases. To our knowledge **5** is the first mononuclear Mn(II) compound featuring an N_3OCl_2 donor set.

Introduction

Catechol metabolism is important both biologically and environmentally. Two major enzymes play the key role in these reactions, catechol dioxygenases and catechol oxidases.[1] Catechol oxidases (which are found in bacteria, fungi, and plants) catalyze the oxidation of a broad range of *o*-diphenols to *o*-quinones.[2] Catechol oxidase is often inferred to be involved in plant defense as highly reactive *o*-quinones autopolymerize to brown polyphenolic catechol melanins, a process that is thought to protect the damaged plant from pathogens or insects. Like hemocyanin and tyrosinase, catechol oxidase is a type three copper enzyme.[3] Crystallographic characterizations of catechol oxidase from sweet potato (*Ipomoea batatas*) revealed the presence of a dinuclear copper center in accordance with that from other plant sources.[4] Therefore, most functional mimics of catechol oxidase are dinuclear Cu(II) complexes, although catalytically active complexes containing other transition metal ions such as Mn, Co, or Ni[5,6] are also known.

Catechol dioxygenases are a part of Nature's strategy for degrading aromatic molecules. They are found in soil bacteria

* To whom correspondence should be addressed: krebs@uni-muenster.de (B.K.); rompela@uni-muenster.de (A.R.); vlpec@umich.edu (V.L.P.).
[†] Institut für Anorganische und Analytische Chemie der Westfälischen Wilhelms-Universität Münster.
[‡] Department of Chemistry, University of Michigan.
[§] Institut für Biochemie der Westfälischen Wilhelms-Universität Münster.

(1) Karlin, K. D., Tyeklár, Z., Eds. *Bioinorganic Chemistry of Copper*; Chapman & Hall: New York, 1993.
(2) Solomon, E. I.; Chen, P.; Metz, M.; Lee, S.-K.; Palmer, A. E. *Angew. Chem.* **2001**, *113*, 4702; *Angew. Chem., Int. Ed.* **2001**, *40*, 4570.
(3) Kaim, W.; Rall, J. *Angew. Chem.* **1996**, *108*, 47; *Angew. Chem., Int. Ed. Engl.* **1996**, *35*, 43.
(4) Klabunde, T.; Eicken, C.; Sacchettini, J. C.; Krebs, B. *Nat. Struct. Biol.* **1998**, *5*, 1084.

10.1021/ic0347788 CCC: $25.00
Published on Web 08/29/2003

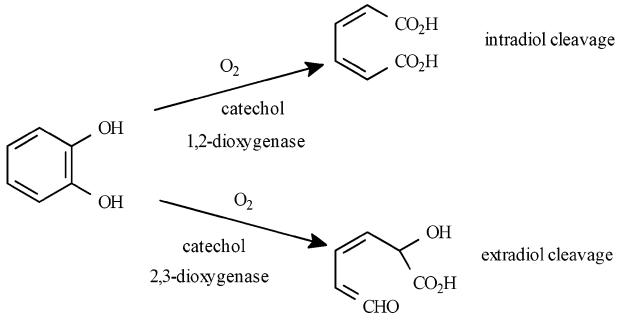

Figure 1. Modes of catechol cleavage catalyzed by catechol 1,2-dioxygenases (intradiol cleavage) and catechol 2,3-dioxygenases (extradiol cleavage).

and act in the last step of transforming aromatic precursors into aliphatic products.[7] Traditionally, catechol dioxygenases are subdivided into two classes, intradiol- and extradiol-cleaving enzymes, according to their ability to catalyze ring cleavage between (intradiol) or outside of (extradiol) the two *ortho*-hydroxo groups (see Figure 1.).[8,9]

Intradiol-cleaving enzymes usually require Fe(III), while the extradiol-cleaving enzymes usually require Fe(II).[10] There are a few examples of extradiol-cleaving enzymes that contain manganese in their active centers.[11−13] A catechol dioxygenase isolated from *Arthrobacter globiformis* CM-2 exists as a homotetramer containing three manganese ions and one iron ion. The importance of the Mn center was established by apoenzyme preparations whose specific activity correlates well with their respective Mn contents and not with their Fe contents.[12] To date there is no crystal structure available of a manganese-dependent catechol dioxygenase. However, a sequence analysis of the enzyme from *Arthrobacter globiformis*[11] is highly homologous to the sequence of the crystallographically characterized iron-dependent extradiol-cleaving catechol dioxygenase from *Pseudomonas cepacia*.[14] The X-ray analysis of the iron enyzme from *P. cepacia* exhibits two histidine ligands and one glutamate ligand while the coordination sphere of Fe(II) is completed by two water molecules. The obtained sequence data indicate that these amino acid residues are conserved in the Mn-containing *A. globiformis*. Therefore, it is a reasonable strategy to prepare structural mimics of Mn-based enzymes given the known structural specifications of the two iron enzyme classes.

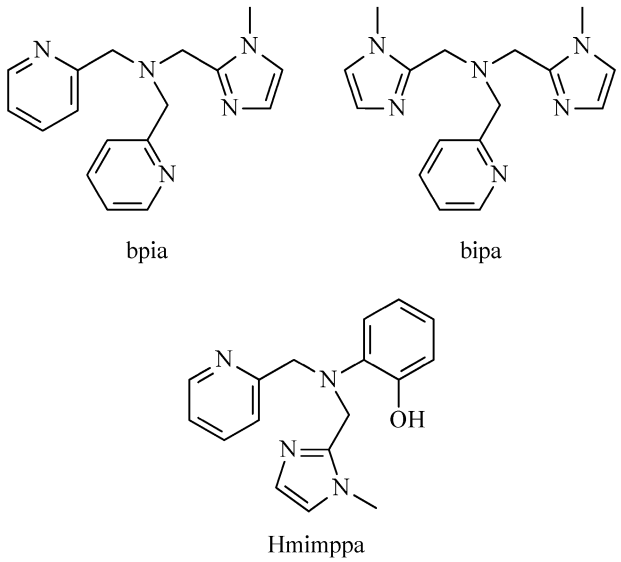

Figure 2. Schematic drawings of the utilized ligands bpia, bipa, and Hmimppa.

In this paper we report the synthesis and structural and spectroscopic characterization of a series of mononuclear manganese compounds that serve to model the chemistry of metal-catalyzed catechol degradation. To mimic the coordination environment of these enzymes, the tetradentate tripodal ligands bis(picolyl)(*N*-methylimidazole-2-yl)amine (bpia),[15] bis(*N*-methylimidazole-2-yl)(picolyl)amine (bipa),[16] and ((1-methylimidazole-2-yl)methyl)((2-pyridyl)methyl)(2-hydroxyphenyl)amine (Hmimppa) were utilized (Figure 2). Notably, the ligands bipa and bpia have also been successfully utilized in the synthesis of Fe-containing functional models of catechol dioxygenase.[15]

Herein, we present a series of novel compounds that are likely to show structural similarity, in terms of the first coordination sphere, to the Mn-substituted catechol dioxygenases. Two of the complexes are structural models for a manganese-substituted form of an intradiol-cleaving iron catechol dioxygenase. While there are no manganese-dependent enzymes of this class known to date, it is possible that such proteins occur since there are many examples of enzymes existing both as iron- and manganese-containing forms (e.g., Mn and Fe SODs).[17] Furthermore, there are both iron and manganese extradiol-cleaving catechol dioxygenases that are known. Four additional compounds containing Mn(III) have been prepared. Two of these have environments that are related to an oxidized form of the Mn extradiol-cleaving catechol dioxygenases. Most interesting, all four Mn(III) compounds reveal high catechol *oxidase* activity using the substrate 3,5-di-*tert*-butylcatchol (3,5-DTBC).

(5) Gultneh, Y.; Farooq, A.; Karlin, K. D.; Liu, S.; Zubieta, J. *Inorg. Chim. Acta* **1993**, *211*, 171.
(6) Kovala-Demertzi, D.; Hadjikakou, S. K.; Demertzis, M. A.; Deligiannakis, Y. *J. Inorg. Biochem.* **1998**, *69*, 223.
(7) Que, L., Jr.; Ho, R. Y. N. *Chem. Rev.* **1996**, *96*, 2607.
(8) Lipscomb, J. D.; Orville, A. M. In *Metal Ions in Biological Systems*; Sigel, A., Sigel, H., Eds.; Marcel Dekker: New York, Basel, 1992**;** Vol. 28, p 243. Senda, T.; Sygiyama, K.; Narita, H.; Yamamoto, T.; Kimbara, K.; Fukuda, M.; Sato, M.; Yano, K.; Mitsui, Y. *J. Mol. Biol.* **1996**, *255*, 735. Ohlendorf, D. H.; Lipscomb, J. D.; Weber, P. C. *Nature (London)* **1988**, *336*, 403. Que, L., Jr. *Iron Carriers and Iron Proteins*; Loehr, T. M., Ed.; VCH: New York, 1989.
(9) Lange, S. J.; Que, L., Jr. *Curr. Opin. Chem. Biol.* **1998**, *2*, 159.
(10) Que, L., Jr.; Reynolds, M. F. In *Metal Ions in Biological Systems*; Sigel, A., Sigel, H., Eds.; Marcel Dekker: New York, Basel, 2000**;** Vol. 37, p 505.
(11) Bolt, Y. R.; Sadowsky, M. J.; Ellis, L. B. M.; Que, L., Jr.; Wackett, L. P. *J. Bacteriol.* **1995**, *177*, 1225.
(12) Whiting, A. K.; Boldt, Y. R.; Hendrich, M. P.; Wackett, L. P.; Que, L., Jr. *Biochemistry* **1996**, *35*, 160.
(13) Que, L., Jr.; Widom, J.; Crawford, R. L. *J. Biol. Chem.* **1981**, *256*, 10941.
(14) Han, S.; Eltis, L. D.; Timmis, K. N.; Muchmore, S. W.; Bolin, J. T. *Science* **1995**, *270*, 976.
(15) Pascaly, M.; Duda, M.; Rompel, A.; Sift, B. H.; Meyer-Klaucke, W.; Krebs, B. *Inorg. Chim. Acta* **1999**, *291*, 289.
(16) (a) Wei, N.; Murthy, N. N.; Tyeklár, Z.; Karlin, K. D. *Inorg. Chem.* **1994**, *33*, 1177. (b) Reese, C. B.; Pei-Zhou, Z. *J. Chem. Soc., Perkin Trans.* **1993**, 2291.
(17) Whittaker, J. W. In *Metal Ions in Biological Systems*; Sigel, A., Sigel, H., Eds.; Marcel Dekker: New York, Basel, 2000; Vol. 37, p 587.

Experimental Section

Physical Measurements. Elemental analyses were performed on a Perkin-Elmer 2400 Series 2 analyzer, an Elementar Vario EL III analyzer, and a Heraeus CHN-O-Rapid analyzer.

IR spectra were recorded on a Perkin-Elmer Spectrum GX FT-IR spectrometer and a Bruker IFS 48 spectrometer in the range of 4000−400 cm^{-1}. Samples were prepared as KBr disks.

UV/vis spectra were measured at 25 °C in acetonitrile (**3**, **4**, **6**) and methanol (**1**−**4**) on a Hewlett-Packard 8453 diode array spectrometer using quartz cuvettes (1 cm). The concentration of the model compounds in methanolic solution was $c = 10^{-3}$ mol·L^{-1} and $c = 5 \times 10^{-4}$ mol·L^{-1} in acetonitrile except for **6**, where a 4.7×10^{-4} mol·L^{-1} solution was used.

EPR spectra were recorded on a Bruker EMX EPR spectrometer at X-band frequency. For low-temperature measurements an Oxford Instruments continuous-flow helium cryostat and a temperature control system were used.

Cyclic voltammetry experiments for compounds **1** and **2** (in methanol) and **5** and **6** (in acetonitrile) were carried out on a Perkin-Elmer 263A potentiostat. The cyclic voltammogram of **4** in acetonitrile was taken on a BAS CV-27 voltammograph equipped with a BAS C-1B cell stand and a BAS RXY recorder; the one for **3** has been reported elsewhere.[18] The concentration of all samples was $c = 1 \times 10^{-3}$ mol·L^{-1}. Prior to use, solvents were purified by standard literature methods.[19] Tetrabutylammonium hexafluorophosphate (recrystallized from ethanol) was used as supporting electrolyte at a concentration of 0.1 mol·L^{-1}. For **3** and **4** a three electrode array consisting of a glassy carbon working electrode, a platinum wire counter electrode, and an $Ag/AgNO_3$ reference electrode, prepared in acetonitrile (0.1 mol·L^{-1} $[Bu_4N][PF_6]$, 0.01 mol·L^{-1} $AgNO_3$), were used. The cyclic voltammograms of compounds **1**, **2**, **5,** and **6** were measured with a Ag/AgCl/3 M NaCl reference electrode. For ease of comparison, all potentials were referenced versus SCE. Using the conditions described above, the ferrocene/ferrocenium redox couple was observed at $E_{1/2} = 0.41$ V vs SCE, at $E_{1/2} = 0.10$ V vs $Ag/AgNO_3$, and at 0.53 V vs Ag/AgCl/3 M NaCl.

Mass spectrometry was performed on Varian MAT 212 and Finnigan MAT 8230 spectrometers.

Kinetic Measurements. The kinetics of the oxidation of 3,5-di-*tert*-butylcatechol (3,5-DTBC) were determined by the method of initial rates. For this purpose 1 mL of 1×10^{-4} M solutions of **1**−**4** in air-saturated methanol was treated with 1 mL of cumulatively concentrated 3,5-DTBC solutions in methanol. The growing band at 400 nm of the product 3,5 di-*tert*-butylquinone (3,5-DTBQ) was monitored by UV/vis spectroscopy as described before.[20] The average initial rates over three independent measurements were determined by linear regression from the slope of the concentration vs time plots. All complexes exhibited saturation kinetics. The data satisfied the Michaelis−Menten equation, originally developed for enzyme kinetics, and the turnover numbers were determined from the double reciprocal Lineweaver−Burk plot[21] (Figure 9).

X-ray Crystallography. The crystal structure of **5** was solved by a Patterson synthesis; all other crystal structures were solved with direct methods using the program system SHELXS 97.[22] All non-hydrogen atoms were taken from a series of full-matrix least-squares refinement cycles based on F^2 with the SHELXL 97 program followed by difference Fourier synthesis.[22] All hydrogen atoms were placed at calculated positions and allowed to ride on their corresponding carbon atoms with isotropic thermal parameters for the methyl protons 1.5 times the value for U_{eq} of the bonding atom and all other hydrogen atoms 1.2 times the value for U_{eq} of the bonding atom. All non-hydrogen atoms were refined anisotropically.

$[Mn(bpia)(OAc)(OCH_3)](PF_6)$ (1). Single crystals were obtained by vapor diffusion of diethyl ether into a methanol solution of **1**. A green crystal with rhombic shape of dimensions $0.40 \times 0.40 \times 0.36$ mm^3 was chosen and mounted onto a Stoe IPDS diffractometer. Unit cell data and diffraction intensities were collected at 213 K using Mo Kα radiation (graphite monochromated, $\lambda = 0.71073$ Å).

$[Mn(bipa)(OAc)(OCH_3)](PF_6)$ (2). Single crystals were obtained by vapor diffusion of diethyl ether into a methanol/acetonitrile solution (1:1) of **2**. A rhombic red crystal of dimensions $0.26 \times 0.10 \times 0.07$ mm^3 was chosen and mounted onto a Bruker AXS SMART diffractometer. Unit cell data and diffraction intensities were collected at 100 K using Cu Kα radiation ($\lambda = 1.54184$ Å).

$[Mn(bipa)(Cl)_2](ClO_4)$ (4). Single crystals were obtained by vapor diffusion of diethyl ether into an acetonitrile solution of **4**. A plate-shaped red crystal of dimensions $0.32 \times 0.28 \times 0.24$ mm^3 was chosen and mounted onto a Stoe IPDS diffractometer. Unit cell data and diffraction intensities were collected at 213 K using Mo Kα radiation (graphite monochromated, $\lambda = 0.71073$ Å).

$[Mn(Hmimppa)(Cl)_2]\cdot CH_3OH$ (5). Single crystals were obtained by vapor diffusion of diethyl ether into an ethanol solution of **5**. A block-shaped, pale yellow crystal of dimensions $0.40 \times 0.24 \times 0.24$ mm^3 was chosen and mounted onto a Stoe IPDS diffractometer. Unit cell data and diffraction intensities were collected at 213 K using Mo Kα radiation (graphite monochromated, $\lambda = 0.71073$ Å).

$[Mn(mimppa)(TCC)]\cdot 2CHCl_3$ (6). Single crystals were obtained by diffusion of *n*-hexane into a $CHCl_3$/DMF solution (1:1) of **6**. A needle-shaped green crystal of dimensions $0.26 \times 0.13 \times 0.11$ mm^3 was chosen and mounted onto a Bruker AXS SMART diffractometer. Unit cell data and diffraction intensities were collected at 100 K using Cu Kα radiation ($\lambda = 1.54184$ Å).

Further crystal data and experimental parameters are listed in Table 1. The crystal structure of $[Mn(bpia)(Cl)_2](ClO_4)$ (**3**) has been reported elsewhere.[18]

Syntheses. bpia (bis(picolyl)(*N*-methylimidazole-2-yl)amine), bipa (bis((1-methylimidazole-2-yl)methyl)((2-pyridyl)methyl)amine), and $[Mn(bpia)(Cl)_2](ClO_4)$ (**3**) were synthesized according to previously reported methods.[15,16,18] All reagents used in the syntheses were purchased from Aldrich and Fluka and used without further purification. All solvents were of analytical grade and used without further purification unless stated otherwise.

Caution! *Perchlorate salts of compounds containing organic ligands are potentially explosive. Only small quantities of these compounds should be prepared and suitable precautionary measures should be taken when they are handled.*

Hmimppa ((1-Methylimidazole-2-yl)methyl)((2-pyridyl)methyl)-(2-hydroxyphenyl)amine. Hppa ((2-pyridylmethyl)(2-hydroxyphenyl)amine)[23−25] (4.0 g, 20 mmol) was dissolved in THF (150 mL)

(18) Triller, M. U.; Hsieh, W.-Y.; Pecoraro, V. L.; Rompel, A.; Krebs, B. *Inorg. Chem.* **2002**, *41*, 5544.
(19) Coetzee, J. F.; *Recommended Methods for Purification of Solvents*: Pergamon: Oxford, U.K., 1982.
(20) Gentschev, P.; Möller, N.; Krebs, B. *Inorg. Chim. Acta* **2000**, *300*, 442.
(21) Lineweaver, H.; Burk, D. *J. Am. Chem. Soc.* **1934**, *56*, 658.
(22) Sheldrick, G. M. *SHELX-97, Program package for Crystal Structure Refinement*; University of Göttingen: Göttingen, Germany, 1997.
(23) Reddig, N.; Triller, M. U.; Pursche, D.; Rompel, A.; Krebs, B. *Z. Anorg. Allg. Chem.* **2002**, *628*, 2458.
(24) Pitt, C. G.; Bao, Y.; Thompson, J.; Wani, M. C.; Rosenkrantz, H.; Metterville, J. *J. Med. Chem.* **1986**, *29*, 1231.

Table 1. Crystal Data and X-ray Experimental Parameters for Complexes **1**, **2**, and **4**−**6**

	1	**2**	**4**	**5**	**6**
formula	$C_{20}H_{25}N_5F_6MnO_3P$	$C_{19}H_{26}N_6F_6MnO_3P$	$C_{16}H_{20}N_6Cl_3MnO_4$	$C_{18}H_{22}N_4Cl_2MnO_2$	$C_{25}H_{19}N_4Cl_{10}MnO_3$
M_r	583.36	586.37	521.67	452.24	832.88
cryst system	triclinic	triclinic	monoclinic	orthorhombic	monoclinic
space group	$P\bar{1}$	$P\bar{1}$	$P2_1/n$	$Pna2_1$	$P2_1/n$
T (K)	213(2)	100(2)	213(2)	213(2)	100(2)
a (Å)	8.872(2)	8.945(2)	9.094(2)	14.345(3)	13.417(3)
b (Å)	11.833(2)	11.336(2)	15.305(3)	15.692(3)	13.930(3)
c (Å)	12.713(3)	12.647(3)	15.865(3)	9.175(2)	17.497(3)
α (deg)	84.57(3)	82.55(3)	90	90	90
β (deg)	73.27(3)	71.63(3)	106.13(3)	90	101.50(3)
γ (deg)	73.97(3)	75.65(3)	90	90	90
V (Å^3)	1228.3(5)	1177.2(4)	2121.2(7)	2065.3(7)	3205(1)
Z	2	2	4	4	4
D_{calc} (g·cm^{-3})	1.577	1.654	1.633	1.451	1.726
μ (mm^{-1})	0.681	5.970	1.037	0.918	11.342
R1 [$I > 2\sigma(I)$][a]	0.0541	0.0544	0.0554	0.0468	0.0447
wR2 [$I > 2\sigma(I)$][b]	0.1365	0.1273	0.1012	0.1099	0.0835
GOF[c]	1.119	0.928	1.019	1.064	0.831

[a] $R1 = \sum||F_o| - |F_c||/\sum|F_o|$. [b] $wR2 = \{\sum[w(F_o^2 - F_c^2)^2]/\sum[w(F_o^2)^2]\}^{1/2}$. [c] $GOF = \{\sum[w(F_o^2 - F_c^2)^2]/n_{data} - n_{vari}\}^{1/2}$.

and 2-(chloromethyl)-1-methylimidazole hydrochloride (5.0 g, 30 mmol) was added, followed by slow addition of triethylamine (6.9 mL, 50 mmol) via a dropping funnel. After the mixture was stirred for 7 days, an off-white precipitate was removed from the reaction mixture by filtration. The resulting brown solution was reduced to a volume of 10 mL and purified by column chromatography (silica, ethyl acetate, methanol), yielding a highly viscous brown oil. Yield: 1.8 g, 31%. Anal. Calcd for $C_{17}H_{18}N_4O$: C, 69.37; H, 6.16; N, 19.03. Found: C, 69.67; H, 6.35; N, 18.83.

[Mn(bpia)(OAc)(OCH$_3$)](PF$_6$) (1). The compound was prepared by reacting equimolar amounts of bpia (0.25 mmol, 74 mg) and $Mn(OAc)_3 \cdot 2H_2O$ (0.25 mmol, 67 mg) in methanol in the presence of acetic acid (0.5 mL). The resulting green solution was stirred for 15 min and filtered to remove unreacted starting material. [Bu$_4$N][PF$_6$] (97 mg, 0.25 mmol) was added, and the resulting reaction mixture was stirred for another 15 min and filtered again. Vapor diffusion of diethyl ether into the filtrate yielded rhombic green crystals suitable for X-ray diffraction. Yield: 93 mg, 65%. Mp: 232 °C. Anal. Calcd for $C_{20}H_{25}N_5F_6MnO_3P$: C, 41.18; H, 4.32; N, 12.01. Found: C, 41.20; H, 4.23; N, 11.93.

[Mn(bipa)(OAc)(OCH$_3$)](PF$_6$) (2). The complex was prepared by reacting equimolar amounts of bipa (0.25 mmol, 74 mg) and $Mn(OAc)_3 \cdot 2H_2O$ (0.25 mmol, 67 mg) in methanol in the presence of acetic acid (0.5 mL). The resulting green solution was stirred for 15 min and filtered to remove unreacted starting material. After addition of [Bu$_4$N][PF$_6$] (97 mg, 0.25 mmol) a green precipitate formed that was collected by filtration and washed with cold methanol. Dissolving the precipitate in a 1:1 mixture of hot methanol and acetonitrile followed by vapor diffusion of diethyl ether into the solution led to the formation of rhombic green crystals suitable for X-ray diffraction. Yield: 88 mg, 61%. Mp: 200−210 °C (dec). Anal. Calcd for $C_{19}H_{26}N_6F_6MnO_3P$: C, 38.92; H, 4.47; N, 14.33. Found: C, 39.03; H, 4.56; N, 14.12.

[Mn(bipa)(Cl)$_2$](ClO$_4$) (4). The complex was prepared by slight modification of a previously published procedure.[26] [Mn(bipa)(OAc)(OCH$_3$)](ClO$_4$) (0.12 mmol, 65 mg) (prepared according to the procedure for **2** using $NaClO_4 \cdot H_2O$ instead of [Bu$_4$N][PF$_6$]) was suspended in methanol, and 2 mL of a 0.12 M solution of HCl in acetonitrile was added. Upon addition of the HCl solution, the green reaction mixture turned into a deep red solution, which was stirred for 5 min and then filtered. Deep red crystals were obtained by vapor diffusion of diethyl ether into the solution. Recrystallization from acetonitrile yielded deep red crystals suitable for X-ray diffraction. Yield: 71 mg, 59%. Mp: 212 °C. Anal. Calcd for $C_{16}H_{20}N_6Cl_3MnO_4$: C, 36.84; H, 3.86; N, 16.11. Found: C, 36.69; H, 3.71; N, 16.10.

[Mn(Hmimppa)(Cl)$_2$]·CH$_3$OH (5). Hmimppa (0.2 mmol, 59 mg) was dissolved in ethanol, and $MnCl_2 \cdot 4H_2O$ (0.2 mmol, 40 mg) was added. The resulting solution was stirred for 30 min and filtered. Vapor diffusion of diethyl ether into the filtrate yielded pale yellow to colorless crystals (depending on the perspective) suitable for X-ray diffraction. Yield: 63 mg, 70%. Mp: 215−220 °C. Anal. Calcd for $C_{18}H_{22}N_4Cl_2MnO_2$: C, 47.81; H, 4.90; N, 12.39. Found: C, 47.64; H, 5.01; N, 12.47.

[Mn(mimppa)(TCC)]·2CHCl$_3$ (6). Tetrachlorocatechol (TCC) (0.1 mmol, 27 mg) was dissolved in a 1:1 mixture of $CHCl_3$ and DMF, and triethylamine (0.3 mmol, 42 μL) was added. [Mn(Hmimppa)(Cl)$_2$]·CH$_3$OH (**5**) (0.1 mmol, 45 mg) was dissolved in a 1:1 mixture of $CHCl_3$ and DMF, and both solutions were combined, resulting in a color change to green. The reaction mixture was stirred for 60 min and filtered. The filtrate was layered with *n*-hexane, yielding green crystals suitable for X-ray diffraction. Yield: 25 mg, 30%. Mp: 220 °C (dec). Anal. Calcd for $C_{25}H_{19}N_4Cl_{10}MnO_3$: C, 36.05; H, 2.30; N, 6.73. Found: C, 35.91; H, 2.40; N, 6.77.

Results and Discussion

Description of Structures. [Mn(bpia)(OAc)(OCH$_3$)](PF$_6$) (1). The crystal structure of the cation in **1** is depicted in Figure 3. Selected bond distances and angles are given in Table 2. Compound **1** crystallizes in the triclinic space group $P\bar{1}$ with two complex cations and two hexafluorophosphate counteranions in the unit cell. The coordination environment around the manganese center can be described as distorted octahedral where nitrogen atoms from bpia occupy four coordination sites and two oxygen atoms from a methoxide and an acetate ligand complete the coordination sphere.

The Mn−N bond distances range from 2.014(3) Å for Mn(1)−N(2) to 2.286(3) Å for Mn(1)−N(1). The distances for the Mn−O bonds are 1.777(3) Å for the methoxide oxygen and 1.955(3) Å for the carboxylate oxygen. These differences

(25) Orr, L. B., Jr.; Parsons, E. J.; Pennington, W. T. *Acta Crystallogr.* **1992**, *C48*, 2042.
(26) Pal, S.; Olmstead, M. M.; Armstrong, W. H. *Inorg. Chem.* **1995**, *34*, 4708.

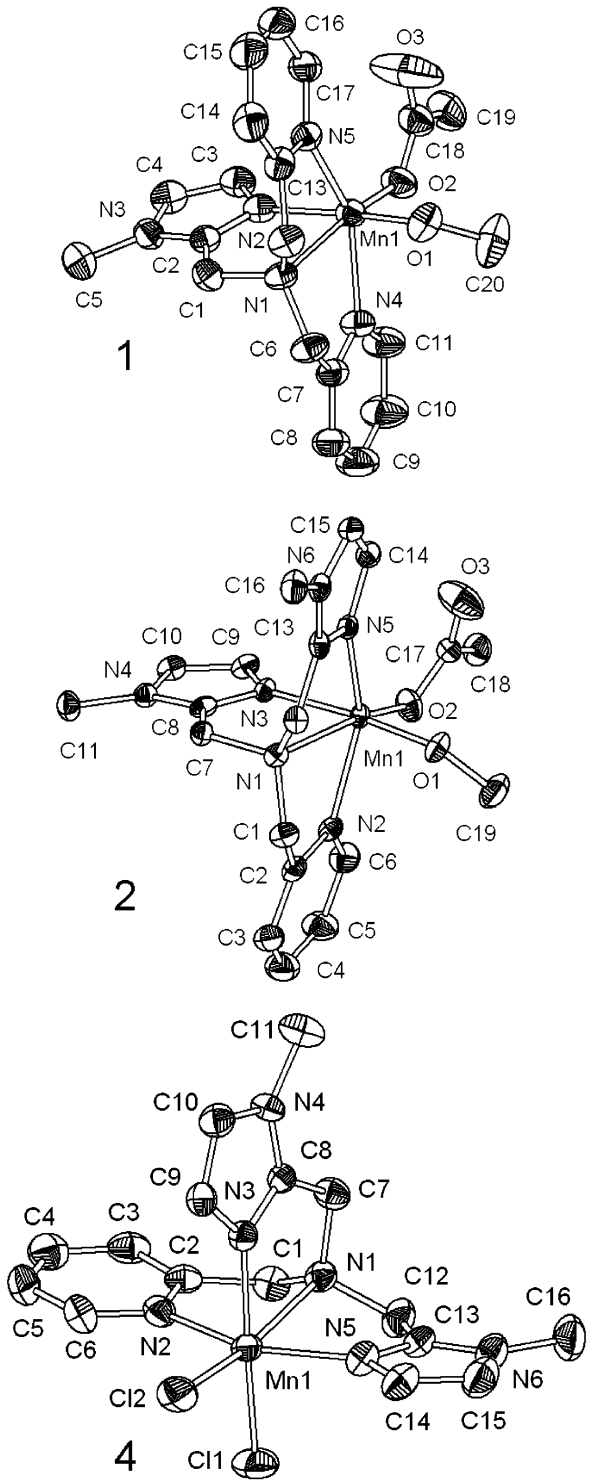

Figure 3. Crystal structures of the cations in **1**, **2**, and **4** showing 50% probability thermal ellipsoids. Hydrogen atoms are omitted for clarity.

in bond lengths are attributed to a rare Jahn−Teller compression along the imidazole nitrogen−manganese−methoxide oxygen axis, arising from the d^4 configuration of the manganese center. It is noteworthy that the carboxylate ligand coordinates in a monodentate fashion as can be seen when comparing the manganese−oxygen distance of 3.156(3) Å for the nonbinding atom O(3) to the bond length of 1.955(3) Å for Mn(1)−O(2). The distortion of the octahedral coordination environment is further manifested in the average N(1)−Mn(1)−N(X) (X = 2, 4, 5) angle of 76.0° which differs significantly from 90°.

[Mn(bipa)(OAc)(OCH$_3$)](PF$_6$) (2). The crystal structure of the cation in **2** is depicted in Figure 3. Selected bond distances and angles are given in Table 2. Like the analogous complex **1**, **2** crystallizes in the monoclinic space group $P\bar{1}$ with two complex cations and two hexafluorophosphate counteranions in the unit cell. The bond distances and angles in **2** (average N(1)−Mn(1)−N(X) (X = 2, 3, 5) angle of 75.6°) resemble the ones in **1** (see Table 2) and also indicate the existence of a rare Jahn−Teller compression along the imidazole nitrogen−manganese−methoxide oxygen axis in **2**. The coordination of the carboxylate ligand in **2** is very similar but not identical to the one in **1**, owing to the different steric demand of the ligands. While in **1** the noncoordinating oxygen atom is almost in plane with the two pyridine arms of bpia and therefore pointing toward the pyridine ring containing N(5), it is directed away from the pyridine ring of bipa in **2** and pointing toward the imidazole ring containing N(5). This results in a greater distance of O(3) from the neighboring aromatic hydrogen atom.

Because of the strong oxophilicity of manganese in higher oxidation states (>+2), the number of mononuclear compounds is very limited. To our knowledge, compounds **1** and **2** are the only mononuclear Mn^{III} complexes with a tripodal ligand and an N_4O_2 donor set. Therefore, these complexes will only be briefly compared to [Mn(BBPEN)](PF$_6$), where the hexadentate ligand BBPEN = *N*,*N*′-bis(2-hydroxybenzyl)-*N*,*N*′-bis(2-methylpyridyl)ethylenediamine contains two phenolate oxygens, two tertiary nitrogens, and two pyridine nitrogen donor atoms.[27] The phenolate oxygen−manganese distances of 1.888(4) and 1.846(4) Å in [Mn(BBPEN)](PF$_6$) fall within the range of manganese−oxygen distances observed for **1** and **2** (see Table 2), while the bonds of the tertiary nitrogen atoms to the manganese center in [Mn(BBPEN)](PF$_6$) are considerably shorter than in **1** and **2** namely 2.124(4) and 2.078(4) Å compared to 2.286(3) and 2.330(3) Å.

[Mn(bipa)(Cl)$_2$](ClO)$_4$ (4). The crystal structure of the cation in **4** is depicted in Figure 3. Selected bond distances and angles are given in Table 2. Compound **4** crystallizes in the monoclinic space group $P2_1/n$ with four complex cations and four perchlorate counteranions in the unit cell. The four nitrogen donor atoms of bipa and the two coordinated chloride ions provide a distorted octahedral coordination environment in **4**. Analogous to **3**[18] the bond lengths for the manganese−chloride bonds with values of 2.224(1) Å for Mn(1)−Cl(1) and 2.362(1) Å for Mn(1)−Cl(2) differ significantly from each other. They are similar to the manganese−chloride distances in [Mn^{III}(bipy)Cl$_3$(H$_2$O)][28] and [Mn(phen)$_2$(Cl)$_2$]NO$_3$·2.5CH$_3$COOH.[29] In the trans position to Cl(2), the tertiary nitrogen atom N(1) is bonded to manganese with a bond length of 2.365(3) Å, which is longer than the distances

(27) Neves, A.; Erthal, S. M. D.; Vencato, I.; Ceccato, A. S.; Mascarenhas, Y. P.; Nascimento, O. R.; Hörner, M.; Batista, A. A. *Inorg. Chem.* **1992**, *31*, 4749.
(28) Tesouro, A.; Corbella, M.; Stoeckli-Evans, H. *Acta Crystallogr.* **1997**, *C53*, 430.
(29) Reddy, K. R.; Rajasekharan, M. V. *Polyhedron* **1994**, *13*, 765.

Table 2. Selected Bond Distances and Angles for Complexes **1**, **2**, and **4**−**6**

	1	**2**	**4**	**5**	**6**
			Bond Distances (Å)		
Mn(1)−O(1)	1.777(3)	1.820(3)		2.294(3)	1.857(3)
Mn(1)−O(2)	1.955(3)	1.969(3)			1.952(3)
Mn(1)−O(3)					1.890(3)
Mn(1)−N(1)	2.286(3)	2.330(3)	2.365(3)	2.367(3)	2.312(3)
Mn(1)−N(2)	2.014(3)	2.225(3)	2.069(3)	2.218(4)	2.128(3)
Mn(1)−N(4)/N(3)[a]	2.243(3)	2.024(3)	2.007(3)	2.283(4)	2.236(3)
Mn(1)−N(5)	2.218(3)	2.163(3)	2.042(3)		
Mn(1)−Cl(1)			2.224(1)	2.398(1)	
Mn(1)−Cl(2)			2.362(1)	2.449(1)	
			Angles (deg)		
O(1)−Mn(1)−O(2)	99.2(1)	99.0(1)			89.5(1)
O(1)−Mn(1)−N_{trans}	171.4(1)	171.0(1)			
O(2)−Mn(1)−N_{trans}	160.4(1)	159.3(1)			164.8(1)
N(1)−Mn(1)−N(2)	79.2(1)	73.8(1)	77.3(1)	73.8(1)	75.0(1)
N(1)−Mn(1)−N(3)/N(4)[a]	74.1(1)	78.6(1)	77.0(1)	71.6(1)	72.9(1)
N(1)−Mn(1)−N(5)	74.6(1)	74.5(1)	75.6(1)		
Cl(1)−Mn(1)−Cl(2)			98.04(4)	104.21(5)	
Cl(1)−Mn(1)−N_{trans}			170.55(8)	162.49(9)	

[a] The atom labels depend on the ligand (cf. Figures 3 and 4).

of 2.069(3) Å for Mn(1)−N(2), 2.007(3) Å for Mn(1)−N(3), and 2.042(3) Å for Mn(1)−N(5). Those donor atoms form the equatorial plane together with Cl(1), while the axis Cl(2)−Mn(1)−N(1) is elongated due to Jahn−Teller distortion. Along the N(2)−Mn(1)−N(5) axis a large distortion from linearity with an angle of 152.8(1)° occurs, which is likely to be caused by the sterically demanding chloride ligands. Similar to **3**, the average N(1)−Mn(1)−N(X) (X = 2, 3, 5) angle of 76.7° differs significantly from 90° due to constraints imposed by the ligand. The corresponding Fe(III) complex $[Fe(bipa)(Cl)_2](ClO_4)$ has been described in the literature.[15] With respect to the nature of the N donor moieties, the largest metal−nitrogen bond distance in this iron compound also occurs between the metal center and the tertiary amine nitrogen atom. As expected for a d^5 transition metal, complex $[Fe(bipa)(Cl)_2](ClO_4)$ exhibits no Jahn−Teller distortion. Hence no significant differences in the metal−chloride bonds were obtained.

$[Mn(Hmimppa)(Cl)_2]\cdot CH_3OH$ (5). The crystal structure of **5** is depicted in Figure 4. Selected bond distances and angles are given in Table 2. Compound **5** crystallizes in the orthorhombic space group $Pna2_1$ with four complex molecules and four methanol molecules in the unit cell. The bond distances for the N_3OCl_2 donor set, which forms a distorted octahedron around Mn(1), vary between 2.218(4) Å for Mn(1)−N(2) and 2.449(1) Å for Mn(1)−Cl(2) and are in very good accordance with other Mn^{II} chloride complexes described in the literature.[30−32] The bond Mn(1)−O(1) is relatively long (2.294(1) Å), which is due to O(1) being protonated. The phenolic hydrogen atom H(1) forms a hydrogen bond to an adjacent methanol molecule with the distance of the donor atom O(1) to the acceptor atom O(2) of 2.607(4) Å. It is noteworthy that the average angle N(1)−

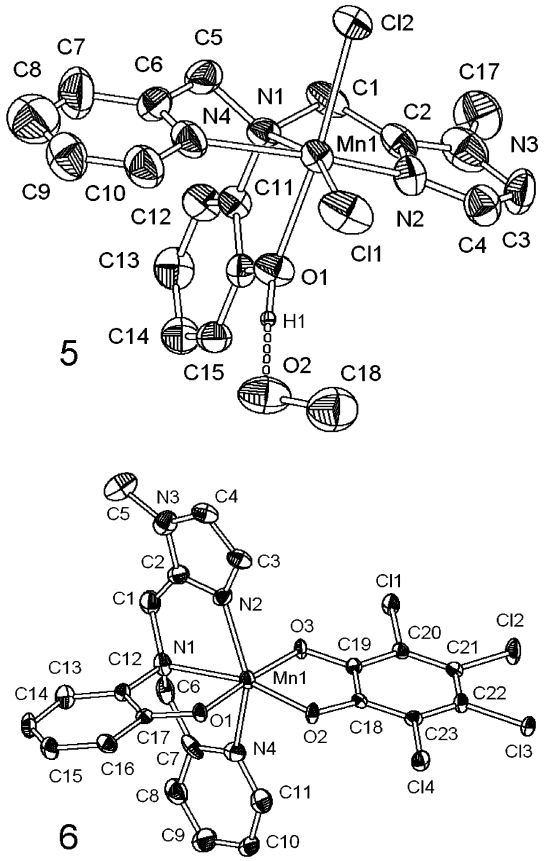

Figure 4. Crystal structures of the neutral Mn complexes in **5** and **6** showing 50% probability thermal ellipsoids. Hydrogen atoms (except H1) are omitted for clarity.

Mn(1)−X (X = N(2), N(4), O(1)) is only 72.8°. This distortion toward the tertiary nitrogen donor atom N(1) is facilitated by the design of the ligand. Although containing a phenol donor arm, Hmimppa exclusively allows for the formation of five-membered chelate rings. It is therefore tailor-made for the synthesis of mononuclear metal complexes with two vacant coordination sites in *cis* position to each other and suppresses the formation of phenoxo-bridged dinuclear complexes. The two coordination sites are occupied

(30) Hubin, T. J.; McCormick, J. M.; Collinson, S. R.; Buchalova, M.; Perkins, C. M.; Alcock, N. W.; Kahol, P. K.; Raghunathan, A.; Busch, D. H. *J. Am. Chem. Soc.* **2000**, *122*, 2512.
(31) Oki, A. R.; Bommarreddy, P. R.; Zhang, H.; Hosmane, N. *Inorg. Chim. Acta* **1995**, *231*, 109.
(32) Sasaki, Y.; Akamatsu, T.; Tsuchiya, K.; Ohba, S.; Sakamoto, M.; Nishida, Y. *Polyhedron* **1998**, *17*, 235.

by the chloride ligands Cl(1) and Cl(2). These enclose a relatively large angle of 104.21(5)° with Mn(1), which is likely to be caused by steric demand and/or electrostatic repulsion. The distortion of the coordination sphere of around Mn(1) can be further shown by calculating the distance of Mn(1) from the three least-squares-planes N(1)/O(1)/Cl(1)/Cl(2), N(1)/N(2)/N(4)/Cl(1), and N(2)/N(4)/O(1)/Cl(2). While this value is only 0.0523 Å for the first plane, it is considerably larger for the second and the third plane, namely 0.2275 and 0.4730 Å.

[Mn(mimppa)(TCC)]·2CHCl$_3$ (6). The crystal structure of **6** is depicted in Figure 4. Selected bond distances and angles are given in Table 2. Compound **6** crystallizes in the monoclinic space group $P2_1/n$ with two complex molecules and eight chloroform molecules in the unit cell. Complex **6** has a distorted octahedral geometry, where the three nitrogen and the three oxygen donor atoms of the N_3O_3 donor set coordinate meridionally to the Mn^{III} center, respectively. The distortion is further reflected in the trans angles of 175.(1)° for O(1)−Mn(1)−O(3), 164.8(1)° for O(2)−Mn(1)−N(1), and 146.9(1)° for N(2)−Mn(1)−N(4). As has been described for **5**, the tripodal ligand causes a distortion of the octahedral coordination sphere toward the tertiary amino group that is visible in the average N(1)−Mn(1)−X (X = N(2), N(4), O(1)) angle of 76.8°. It is remarkable that the tetrachlorocatecholate ligand is asymmetrically coordinated. With 1.952(3) Å the bond Mn(1)−O(2) is 0.06 Å longer than Mn(1)−O(3). Examination of the bond lengths within the tetrachlorocatecholate ligand leads to the result that it exists in the catecholate and not in the semiquinonate form. Although the bond C(18)−C(19) is slightly longer than the other C−C bonds in the aromatic ring, this is not unusual and has been reported for other catecholate complexes.[33,34] The bond lengths of 1.331(4) and 1.345(4) Å for O(2)−C(18) and O(2)−C(19) are characteristic of the catecholate form, while, for the semiquinonate form, an average bond length of 1.29 Å would be expected.[35] Besides [Mn(cth)(3,5-DTBC)](BPh$_4$),[36] **6** is the only mononuclear manganese catecholate complex with a stoichiometry of metal:ligand:catechol = 1:1:1, whereas a number of [Mn(L)$_n$(catechol)$_2$] and [Mn(catechol)$_3$] complexes are known.[37,38]

Electronic Spectra and Mass Spectrometry. The electronic spectra of complexes **1**−**4** are depicted in Figure 5. The UV/vis spectrum of **5** shows no bands due to the ^{6}S ground state of the Mn^{II} center. The UV/vis spectrum of **6** is depicted in Figure 6. Band positions and extinction coefficients are summarized in Table 3. The optical spectra of **1** and **2** are almost identical (Figure 5, top). In methanol bands originate from d−d transitions at 409 nm (268 M^{-1} cm^{-1}) and 731 nm (64 M^{-1} cm^{-1}) for **1** and 410 nm (282 M^{-1} cm^{-1}) and 731 nm (67 M^{-1} cm^{-1}) for **2**. With the help of mass spectrometry (peaks at m/z = 438 and 441, respectively), the species in solution were identified to have the general formula $[Mn(L)(OMe)(OAc)]^+$. The broad bands at higher wavelength are comparable to absorption bands found for the two dinuclear manganese complexes [Mn$_2$-

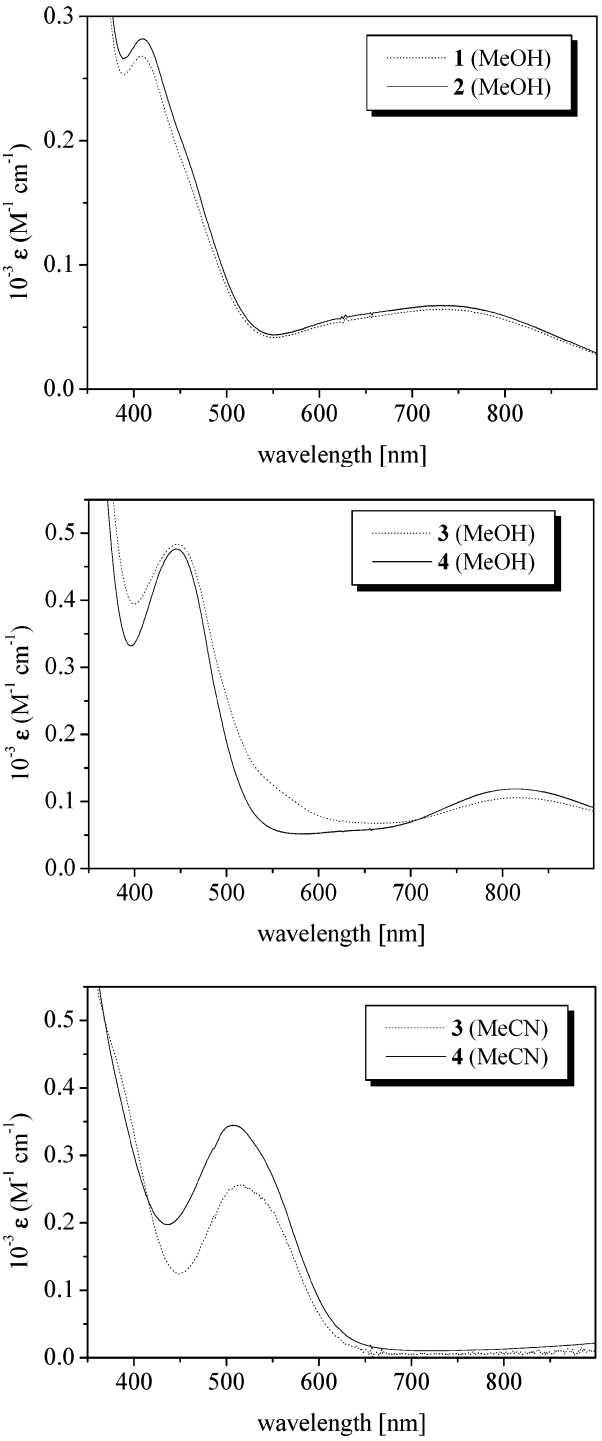

Figure 5. Electronic spectra of complexes **1** and **2** in methanol (top), **3** and **4** in methanol (middle), and **3** and **4** in acetonitrile (bottom).

(33) (a) Que, L., Jr.; Kolanczyk, R. C.; White, L. S. *J. Am. Chem. Soc.* **1987**, *109*, 5373. (b) Cox, D. D.; Que, L., Jr. *J. Am. Chem. Soc.* **1988**, *110*, 8085. (c) Jang, H. G.; Cox, D. D.; Que, L., Jr. *J. Am. Chem. Soc.* **1991**, *113*, 9200.
(34) Pierpont, C. G.; Lange, C. W. *Prog. Coord. Chem.* **1993**, *41*, 381.
(35) Adams, M.; Dei, A.; Rheingold, A. L.; Hendrickson, D. N. *J. Am. Chem. Soc*. **1993**, *115*, 8221.
(36) Caneschi, A.; Dei, A. *Angew. Chem.* **1998**, *110*, 3220; *Angew. Chem., Int. Ed. Engl.* **1989**, *28*, 3005.
(37) Larsen, S. K.; Pierpont, C. G.; DeMunno, G.; Dolcetti, G. *Inorg. Chem.* **1986**, *25*, 4828.
(38) (a) Hartman, J. A. R.; Foxman, B. M.; Cooper, S. R. *J. Chem. Soc., Chem. Commun.* **1982**, 583. (b) Hartman, J. A. R.; Foxman, B. M.; Cooper, S. R. *Inorg. Chem.* **1984**, *23*, 1381. (c) Ruiz, R.; Caneschi, A.; Gatteschi, D.; Sangregorio, C.; Sorace, L.; Vazquez, M. *Inorg. Chem. Commun.* **2000**, *3*, 76.

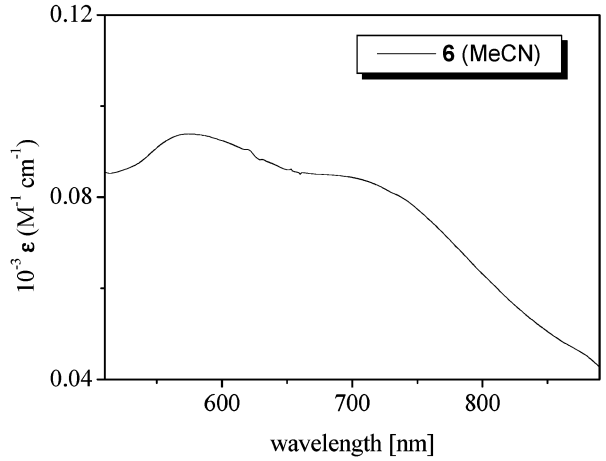

Figure 6. Electronic spectrum of complex **6** in acetonitrile.

Table 3. UV/vis Data for Complexes **1**−**6**

complex	λ_{max} (nm) (ϵ (M^{-1}·cm^{-1}))
1	409 (268), 731(64)
2	410 (282), 731 (67)
3 (in MeOH)	447 (483), 816 (106)
4 (in MeOH)	445 (476), 813 (119)
3 (in MeCN)[18]	377 (918), 514 (512)
4 (in MeCN)	508 (688)
6	362 (3695), 577 (201), 710 (178)

$(bpia)_2(\mu\text{-}O)(\mu\text{-}OAc)](ClO_4)_3{\cdot}CH_3CN$ and $[Mn_2(TMIMA)_2(\mu\text{-}O)(\mu\text{-}OAc)](ClO_4)_3{\cdot}2CH_3CN$,[18,39] whose absorption bands are also centered in this region. This similarity among the electronic absorption spectra can be explained by the analogous first coordination spheres of the four complexes, which are comprised of two oxygen donor atoms from the ancillary ligands acetate and oxide or methoxide as well as four nitrogen donor atoms, namely one aliphatic nitrogen atom and three nitrogen donor atoms from pyridine and/or methylimidazole. The UV/vis spectra of **3** and **4** in identical solvents also resemble each other while there are differences when different solvents are used (Figure 5). In methanol, bands are found at 447 and 816 nm (483, 106 M^{-1} cm^{-1}, respectively) for **3** and at 445 and 813 nm (476, 119 M^{-1} cm^{-1}, respectively) for **4**. The extinction coefficients, given in parentheses, suggest that these are d−d transitions. In acetonitrile, the UV/vis spectra of **3** and **4** exhibit bands at 514 nm (512 M^{-1} cm^{-1}) and 508 nm (688 M^{-1} cm^{-1}), respectively, which can be attributed to d−d transitions in accordance with the literature.[40] In addition, a shoulder at 377 nm (918 M^{-1} cm^{-1}) can be found in the spectrum of **3**. A comparison with two iron complexes described in the literature leads to the conclusion that this shoulder is due to a LMCT transition from chloride to the Mn^{III} center.[15,41] The differences in the spectra of **3** and **4** taken in both methanol and acetonitrile have been further probed by mass spectrometry and have been found to originate from ligand displacement by solvent molecules. In acetonitrile, **3** and **4** exist as monocations with the general formula $[Mn(L)(Cl)_2]^+$ (L = bpia, bipa) as shown by peaks at m/z = 418−423 (isotope cluster) and m/z = 421−426 (isotope cluster), respectively, while, in methanol, one chloride ligand is substituted with a methanol solvent molecule. Peaks at m/z = 414−417 (isotope cluster) and m/z = 417−420 (isotope cluster) for **3** and **4**, respectively, are indicative of the general formula $[Mn(L)(Cl)(MeOH)]^{2+}$ (L = bpia, bipa). Complexes **3** and **4** are the chloride substituted analogues of **1** and **2**. In accordance with the spectrochemical series, the effect of the substitution of two oxygen donor ligands, namely methoxide and acetate for two chloride ligands, results in a band shift originating from d−d transitions by approximately 100 nm (cf. Table 3 and Figure 5).

The UV/vis spectrum of **6** exhibits a charge-transfer band from a phenolic oxygen p_π-orbital into a manganese centered d_π^* orbital at 362 nm with an extinction coefficient of 3695 M^{-1} cm^{-1}. Additionally bands at 577 and 710 nm can be observed (cf. Figure 6 and Table 3). On the basis of their extincition coefficients (201 and 178 M^{-1} cm^{-1}, respectively), these bands are attributed to d−d transitions. The absence of pronounced bands in the region between 770 and 910 nm supports the conclusion that the TCC ligand has no semiquinone character.[42,43]

Electrochemistry. Cyclic voltammograms for complexes **1**, **2**, and **4**−**6** are depicted in Figure 7. Redox potentials are summarized in Table 4. All values are given versus SCE. The electrochemistry of **3** has been reported elsewhere.[18] A solution of complex **1** in methanol displays a quasi-reversible one electron redox process at $E_{1/2}$ = −0.24 V with ΔE = 180 mV, corresponding to the Mn^{II}/Mn^{III} redox couple and another one at $E_{1/2}$ = 0.79 V with ΔE = 130 mV, originating from the Mn^{III}/Mn^{IV} redox couple. A small broad peak around 0.03 V is most likely due to a very small amount of the dinuclear species $[Mn_2(bpia)_2(\mu\text{-}O)(\mu\text{-}OAc)]^{3+}$.[18] Analogous to **1**, **2** displays two quasi-reversible transitions at $E_{1/2}$ = −0.27 V with ΔE = 150 mV and at $E_{1/2}$ = 0.79 V with ΔE = 130 mV. Here, a small broad peak is observed at −0.02 V that is most likely assigned to the dinuclear species $[Mn_2(bipa)_2(\mu\text{-}O)(\mu\text{-}OAc)]^{3+}$. In the cyclic voltammogram of **4**, two quasi-reversible redox processes for the Mn^{II}/Mn^{III} and the Mn^{III}/Mn^{IV} redox couple can be observed at $E_{1/2}$ = 0.60 V (ΔE = 120 mV) and $E_{1/2}$ = 1.44 (ΔE = 100 mV), which compares well with the electrochemistry of **3**.[18] Compared to the latter complex, the potentials in **4** are only slightly shifted to lower values, reflecting the small difference in donor strength of the two ligands bpia and bipa. In good agreement with the literature it is noteworthy that a substitution of oxygen donor atoms by chloride ligands causes a notable shift of the redox potential toward higher values.[18,44] For **5**, two quasi-reversible peaks at $E_{1/2}$ = 0.88 V with ΔE = 150 mV and $E_{1/2}$ = 1.20 V with ΔE = 140 mV can be

(39) Oberhausen, K. J.; O'Brien, R. J.; Richardson, J. F.; Buchanan, R. M.; Costa, R.; Latour, J.-M.; Tsai, H.-S.; Hendrickson, D. N. *Inorg. Chem.* **1993**, *32*, 4561.
(40) Dingle, R. *Acta Chem. Scand.* **1966**, *20*, 33.
(41) Kojima, T.; Leising, R. A.; Yan, S.; Que, L., Jr. *J. Am. Chem. Soc.* **1993**, *115*, 11328.
(42) Benelli, C.; Dei, A.; Gatteschi, D.; Pardi, L. *Inorg. Chem.* **1989**, *28*, 1476.
(43) Lynch, M. W.; Hendrickson, D. N.; Fitzgerald, B. J.; Pierpont, C. G. *J. Am. Chem. Soc.* **1984**, *106*, 2041.
(44) Horner, O.; Anxolabéhère-Mallart, E.; Charlot, M.-F.; Tchertanov, L.; Guilhem, J.; Mattioli, T. A.; Boussac, A.; Girerd, J.-J. *Inorg. Chem.* **1999**, *38*, 1222.

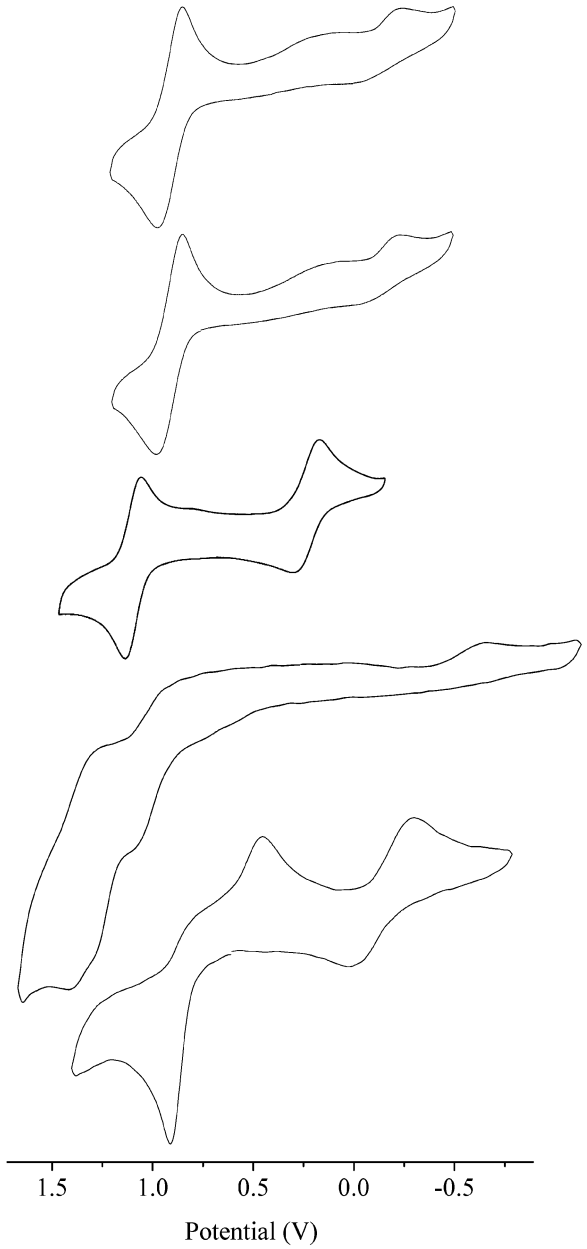

Figure 7. Cyclic voltammograms of complexes **1** and **2** in methanol and **4**−**6** in acetonitrile.

Table 4. Redox Potentials of Complexes **1**−**6**

	$E_{1/2}$ (ΔE) (V versus Ag/AgCl)	
complex	Mn^{II}/Mn^{III}	Mn^{III}/Mn^{IV}
1	−0.24 (0.18)	0.79 (0.13)
2	−0.27 (0.15)	0.79 (0.13)
3	0.61 (0.09)[a,18]	1.53 (0.09)[a,18]
4	0.60 (0.12)[a]	1.53 (0.10)[a]
5	0.88 (0.15)	1.20 (0.14)
6	−0.27 (0.30)[b]	0.80/0.35[c]

[a] Versus $Ag/AgNO_3$. [b] Semiquinonate−catecholate transition. [c] Semiquinonate−quinone transition; irreversible.

found which correspond to the redox couples Mn^{II}/Mn^{III} and Mn^{III}/Mn^{IV}, respectively. Complex **6** shows one irreversible and one quasi-reversible redox process. By comparison to the cyclic voltammetry data given in the literature for other transition metal TCC compounds[35,45] and transition metal 3,5-DTBC compounds[46] and in accordance with those reports, the following tentative assignments can be made. The irreversible peaks at an anodic potential of 0.80 V and a cathodic potential of 0.35 V correspond to the semiquinonate−quinone transition of the bound ligand, while the quasi-reversible peak at $E_{1/2} = -0.27$ ($\Delta E = 0.30$ V) stems from semiquinonate−catecholate transition.

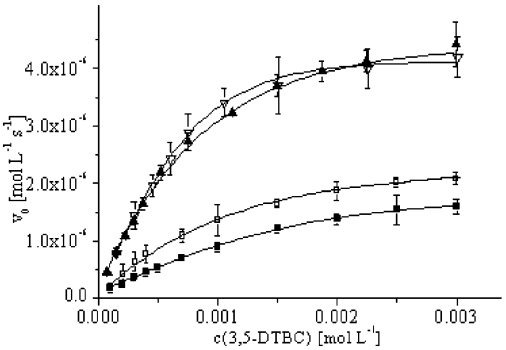

Figure 8. Initial rate of 3,5-DTBQ formation versus 3,5-DTBC concentration at constant concentration of catalyst (solid squares, **1**; open squares, **2**; solid triangles, **3**; open triangles, **4**; lines, corresponding curve fit).

Kinetic Investigations. Air-saturated methanol solutions of **1**−**5** (1×10^{-4} M) were treated with 10 equiv of 3,5-DTBC. No base was added to the solutions to suppress an oxidation of the substrate by base. The first apparent result, while the reaction by UV/vis spectroscopy was monitored, is a significant difference in the reactivity of the complexes **1**−**4**. These compounds show a remarkable activity, namely a formation of a band at 400 nm which is indicative of a oxidation from 3,5-di-*tert*-butylcatchol to 3,5-di-*tert*-butyl-*o*-quinone (a decreasing band around 600 nm implicates that no semiquinone as byproduct is formed) while complex **5** exhibits no catalytic activity. Consequently, the catecholase activity of complexes **1**−**4** was studied. As depicted in Figure 8 all four complexes show saturation kinetics at high substrate concentrations. Complex **3** was found to have the highest catalytic activity followed by complex **4**. The turnover numbers were determined as $k_{cat} = 230 \pm 4$ h^{-1} and $k_{cat} = 130 \pm 7$ h^{-1}, respectively. For the remaining two catalytically active compounds **1** and **2** turnover numbers of $k_{cat} = 86 \pm 7$ h^{-1} and $k_{cat} = 101 \pm 4$ h^{-1}, respectively, were calculated. The Lineweaver−Burk-plots are depicted in Figure 9. The determined kinetic data for **1**−**4** place these compounds into the upper range of functional models for catecholase active complexes. Further kinetic data are summarized in Table 5.

Both chloride-containing Mn(III) complexes **3** and **4** exhibit higher oxidation rates comparable to the correspond-

(45) Benelli, C.; Dei, A.; Gatteschi, D.; Güdel, H. U.; Pardi, L. *Inorg. Chem.* **1989**, *28*, 3089.
(46) Cox, D. D.; Que, L., Jr. *J. Am. Chem. Soc.* **1988**, *110*, 8085.
(47) Gentschev, P.; Möller, N.; Krebs, B. *Inorg. Chim. Acta* **2000**, *300*, 442.
(48) Murthy, N. N.; Karlin, K. D.; Bertini, I.; Luchinat, C. *J. Am. Chem. Soc.* **1997**, *119*, 2156.
(49) Neves, A.; Rossi, L. M.; Vencato, I.; Drago, V.; Haase, W.; Werner, R. *Inorg. Chim. Acta* **1998**, *281*, 111.
(50) Neves, A.; Rossi, L. M.; Horn, A., Jr.; Vencato, I.; Bortoluzzi, A. J.; Zucco, C.; Mangrich, A. S. *Inorg. Chem. Commun.* **1999**, *8*, 334.
(51) Reim, J.; Krebs, B. *J. Chem. Soc., Dalton Trans.* **1997**, 3793.

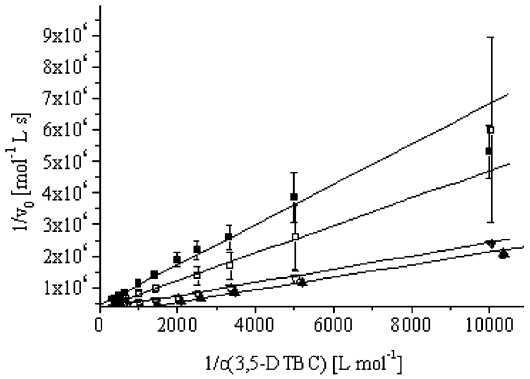

Figure 9. Lineweaver−Burk plot (solid squares, **1**; open squares, **2**; solid triangles, **3**; open triangles, **4**).

Table 5. Catalytic Activity of Synthetic Catecholase Mimics

compd	k_2 (h^{-1})	K_M (mM)	k_{cat}/K_M ($s^{-1}\cdot M^{-1}$)	ref
1	86	1.5	16	
2	101	1.2	23	
3	230	1.3	49	
4	130	0.8	45	
$[Mn(diclofenac)_2(H_2O)]^{a,b}$	225			6
$[Mn(tpa)_2](ClO_4)_2^{a,c}$	4			5
$[Cu_2(L^1)(\mu\text{-OAc})](ClO_4)_2^{a,d}$	3.9			47
$[Cu_2(L^2)_2](PF_6)_2^{a,e}$	5.1			47
$[Cu_2(P1\text{-}O)(OAc)](ClO_4)_2^{f}$	10	0.86	3.3	48
$[Cu_2(H_2bbppnol)(\mu\text{-Oac})(H_2O_2)]Cl_2^{g}$	28	0.79	10	49
$[Cu_2(Hbtppnol)(\mu\text{-OAc})](ClO_4)_2^{h}$	28	0.95	8.1	50
$[Cu_2(L^3)_2(CH_3CN)_2](PF_6)_2^{a,i}$	31.6			47
$[Cu_2(L^4)(OH)(EtOH)(H_2O)](ClO_4)_2^{k}$	214	0.24	248	51

[a] No saturation kinetics observed/reported. [b] diclofenac = (2-((2,6-dichlorophenyl)amino)phenyl)acetate. [c] tpa = tris(2-pyridylmethyl)amine. [d] L^1 = *N*,*N*,*N*′,*N*′-tetrakis(*N*-(2-hydroxyethyl)-2-benzimidazolylmethyl)-2-hydroxy-1,3-diaminopropane. [e] L^2 = (2-hydroxybenzyl)(*N*,*N*′-dimethylpropyl)amine. [f] P1-OH = 1,3-bis(bis(2-pyridylmethyl)amino)propanol. [g] H_3bbppnol = *N*,*N*′-bis(2-hydroxybenzyl)-*N*,*N*′-bis(pyridylmethyl)-2-hydroxy-1,3-propandiamine. [h] H_2btppnol = *N*-(2-hydroxybenzyl)-*N*,*N*,*N*′-tris(2-pyridylmethyl)-1,3-diaminopropan-2-ol. [i] L^3 = (2-pyridylmethyl)(1-hydroxypropyl)amine. [k] L^4 = 4-bromo-2,6-bis(4-methylpiperazin-1-ylmethyl)-phenol.

ing complexes **1** and **2** although the coordination sphere of **1** and **2** enclose one acetate and one methanolate ligand each. This is noteworthy, if one presumes a coordination of 3,5-DTBC as a mono- or dianion during the catalytic cycle. Both acetate and methanolate should benefit by a deprotonation of the substrate. This should accelerate the necessary binding of the deprotonated substrate to the metal center and should lead to higher initial rates. Since the chloride-substituted compounds exhibit the highest catalytic activity, the ease of substitution of the terminal ligands seems to be the rate-determining step. As described above, it has been proven by UV/vis spectroscopy and mass spectrometry that **3** and **4** both exist as different cationic species depending on the solvent. In methanol, one chloride ligand is replaced by a solvent molecule leading to an $[Mn(L)(Cl)(MeOH)]^{2+}$ species (L = bpia or bipa, respectively). In these higher charged complexes the coordinated methanol might be replaced more easily by the substrate yielding a higher activity. In contrast, the UV/vis spectra of compounds **1** and **2** in methanol indicate that both complexes remain as monocationic compounds in solution without the substitution of any labile ligand.

No systematic influences based upon the respective tripodal ligands were found; however, a correlation between the rate of oxidation and the compounds' $E_{1/2}$ values was obtained. The easier the catalyst is reduced, the higher is its catalytic activity. This is in good agreement with data given in the literature for $[M^{II}(diclofenac)_2H_2O)]$ complexes (M = Mn, Co, Ni, Cu),[6] where the manganese complex was found to have the highest catalytic activity regarding the oxidation of 3,5-DTBC and was also the most reducible compound.

Conclusion

With the tripodal ligands bpia and bipa, manganese compounds that are structurally related to the proposed active site of manganese-dependent extradiol-cleaving catechol dioxygenase have been synthesized and structurally characterized. Complexes **1**−**4** exhibit high catalytic activity for the oxidation of 3,5-di-*tert*-butylcatechol to 3,5-di-*tert*-butylquinone. They belong to the class of synthetic catechol oxidase model compounds showing saturation kinetics at high substrate concentrations. Unfortunately, it is unclear what precise role the redox potential plays in the mechanism of oxygen activation by iron- and manganese-dependent extradiol-cleaving dioxygenases. However, a clear correlation between the redox potential and the catechol oxidase like catalytic activity was revealed for our model oxidation reactions. For compounds **1**−**4** the redox potential is not appropriate to allow catechol cleavage; however, these compounds are capable of performing an oxidation to the corresponding quinone. It is noteworthy that within the proposed mechanism for extradiol cleavage of catechol a (semi)quinone-like intermediate is presumed.[7] Therefore, compounds **1**−**4** represent the first step to develop synthetic manganese model compounds that can act as extradiol-cleaving catechol mimics.

Compounds **5** and **6** can be regarded as structural models for a manganese-substituted intradiol-cleaving catechol dioxygenases. To our knowledge, **5** is the first mononuclear Mn(II) compound featuring an N_3OCl_2 donor set.

Acknowledgment. Financial support by the BMBF and DFG is gratefully acknowledged. A.R. and B.K. thank the FCI (Fonds der Chemischen Industrie) for financial support, and M.U.T. is thankful for a Doktorandenstipendium. V.L.P. thanks the NIH (Grant GM39406) and the Alexander von Humboldt award for senior U.S. scientists for financial support.

Supporting Information Available: CIF files of complexes **1**, **2**, and **4**−**6**, IR, mass spectrometry, ^{1}H NMR, and ^{13}C NMR data for the ligand Hmimppa, and IR and mass spectrometry data for complexes **1**, **2**, and **4** as well as IR data for complexes **5** and **6** and the EPR spectrum of **5**. This material is available free of charge via the Internet at http://pubs.acs.org.

IC0347788